Available online at www.sciencedirect.com
SCIENCE DIRECT®
Journal of Sound and Vibration 288 (2005) 361–373
JOURNAL OF SOUND AND VIBRATION
www.elsevier.com/locate/jsvi

Symmetric wave propagation in a fluid-saturated incompressible porous medium

Rajneesh Kumar[a,*], B.S. Hundal[b]

[a]*Department of Mathematics, Kurukshetra University, Kurukshetra, Haryana 136-119, India*
[b]*Department of Mathematics, S.R. Government College for Women, Amritsar, Punjab, India*

Received 11 November 2002; received in revised form 12 January 2004; accepted 26 August 2004
Available online 20 April 2005

Abstract

A study of symmetric wave propagation in a fluid-saturated incompressible porous medium is presented. The governing equations are solved by the method of characteristics. Characteristic equations and the relations for discontinuities across the wave fronts are derived and Heaviside step input function is taken for the numerical investigation.

1. Introduction

The problems related to fluid-saturated porous media are attracting more and more attention because of their significance in the field of geophysics, soil-mechanics and other such field of engineering. So many porous media theories have been presented. Biot theory [1] is based on the assumption of compressible constituents and propagation of two dilatational and one rotational waves have been concluded. Another interesting theory is given by Bowen [2] and Boer and Ehlers [3]. In this theory, all the constituents of a porous medium are assumed to be incompressible. One-dimensional transient wave propagation in fluid-saturated incompressible porous media has been discussed by Boer and Ehlers [4]. The saturating fluid is assumed to be inviscid and the

*Corresponding author.
E-mail address: rajneesh_kuk@rediffmail.com (R. Kumar).

0022-460X/$ - see front matter © 2004 Elsevier Ltd. All rights reserved.
doi:10.1016/j.jsv.2004.08.046

incompressibility constraint exhibits only one independent dilatational wave propagating in both the solid and fluid phases.

In this paper, we have discussed the propagation of symmetric waves in a fluid-saturated incompressible porous medium. The porous medium is modeled as a two-phase system composed of incompressible solid and fluid phases, where the general field equations are directly adopted as the work of Boer and Ehlers [3]. The method of characteristics is applied to solve the governing equations. The advantage of this method is that, it gives the simple description of wave fronts, path of waves and can be used for arbitrary input functions. The method of characteristics for one space variable has been successfully used by many investigators [5–13] and [14–16] have applied this method for two space variables where these authors have sufficiently discussed the numerical integration along the bi-characteristic lines. Ideas used by these authors are given in the standard texts [17–20]. The numerical integration procedure along the characteristic directions is simple, stable and is rapidly convergent. Sneddon [20] has presented another important property of this method describing the fact that if there is a discontinuity at any point of a characteristic curve, then there must be one at all the points of this curve. It is this property which identifies a characteristic curve as a wave front. So following this method, the analytical results for discontinuities across the wave front are obtained and Heaviside unit step input is taken for numerical investigation.

2. Basic equations

Within the framework of modern porous media theory [3], the equations governing the deformation of an incompressible porous medium are

$$\operatorname{div}(\eta^S \dot{\mathbf{x}}_S + \eta^F \dot{\mathbf{x}}_F) = 0, \tag{1}$$

$$\operatorname{div} \mathbf{T}_E^S - \eta^S \operatorname{grad} p + \rho^S(\mathbf{b} - \ddot{\mathbf{x}}_S) - \mathbf{P}_E^F = 0, \tag{2}$$

$$\operatorname{div} \mathbf{T}_E^F - \eta^F \operatorname{grad} p + \rho^F(\mathbf{b} - \ddot{\mathbf{x}}_F) + \mathbf{P}_E^F = 0, \tag{3}$$

where $\dot{\mathbf{x}}_i$ and $\ddot{\mathbf{x}}_i$ $(i = F, S)$ denote the velocities and accelerations of solid and fluid phases, respectively, and p is the effective pore pressure of the incompressible pore fluid. ρ^S and ρ^F are the densities of the solid and fluid phases, respectively, and $\mathbf{b}$ is the body force per unit volume. $\mathbf{T}_E^S$, $\mathbf{T}_E^F$ and $\mathbf{P}_E^F$ are called the extra quantities for which the constitutive equations must be formulated and η^S, η^F are the volume fractions satisfying

$$\eta^S + \eta^F = 1. \tag{4}$$

If $\mathbf{u}_S$ and $\mathbf{u}_F$ are the displacement vectors for solid and fluid phases then

$$\dot{\mathbf{x}}_S = \dot{\mathbf{u}}_S, \quad \ddot{\mathbf{x}}_S = \ddot{\mathbf{u}}_S, \quad \dot{\mathbf{x}}_F = \dot{\mathbf{u}}_F, \quad \ddot{\mathbf{x}}_F = \ddot{\mathbf{u}}_F. \tag{5}$$

The investigations to follow are restricted to an isotropic, linear elastic porous solid filled with an inviscid liquid. So the constitutive equations for extra stresses and extra momentum are given by de Boer and Ehlers [3] as

$$\mathbf{T}_E^S = 2\mu^S \mathbf{E}_S + \lambda^S(\mathbf{E}_S.\mathbf{I})\mathbf{I}, \tag{6}$$

$$\mathbf{T}_E^F = 0, \tag{7}$$

$$\mathbf{P}_E^F = -\mathbf{S}_V(\dot{\mathbf{u}}_F - \dot{\mathbf{u}}_S), \tag{8}$$

where λ^S and μ^S are the macroscopic Lame's constants of the porous solid and $\mathbf{E}_S$ is the linearized Langrangian strain tensor defined as

$$\mathbf{E}_S = \tfrac{1}{2}(\text{grad}\,\mathbf{u}_S + \text{grad}^{\mathrm{T}}\,\mathbf{u}_S). \tag{9}$$

In the case of isotropic permeability, the tensor $\mathbf{S}_V$, describing the coupled interaction between the solid and fluid is given by Boer and Ehlers [3] as

$$\mathbf{S}_V = \frac{(\eta^F)^2\gamma^{\mathrm{FR}}}{K^F}\mathbf{I}, \tag{10}$$

where γ^{FR} is the effective specific weight of the fluid and K^F is the Darcy's permeability coefficient of the porous medium.

3. Formulation of the problem

We consider an infinite fluid-saturated incompressible porous medium having a cavity (spherical or cylindrical) of radius r_0. Initially the surface $r = r_0$ is not loaded. So each particle of the medium is at rest. As time progresses, a time-dependent input $f(t)$ is applied at $r = r_0$ either suddenly or gradually. In the scope of infinitesimal deformation, all the terms of higher order are neglected. Moreover, the small variation in the volume fractions is also neglected. So considering the motion to be spherically (cylindrically) symmetric, taking body forces to be absent and after using Eqs. (5) and (7); we can write Eqs. (1)–(3) as

$$\eta^S\frac{\partial v^S}{\partial r} + \eta^F\frac{\partial v^F}{\partial r} = 0, \tag{11}$$

$$\frac{\partial \tau_r}{\partial r} + \frac{N}{r}(\tau_r - \tau_\theta) - \eta^S\frac{\partial p}{\partial r} + S_V(v^F - v^S) = \rho^S\frac{\partial v^S}{\partial t}, \tag{12}$$

$$-\eta^F\frac{\partial p}{\partial r} - S_V(v^F - v^S) = \rho^F\frac{\partial v^F}{\partial t}, \tag{13}$$

where τ_r, τ_θ are the components of stress on the porous solid, v^S, v^F are the only non-zero components of velocities of solid and fluid particles respectively, and N is a constant and its value is zero for plane wave, one for cylindrical wave and two for spherical wave. Also Eqs. (6) and (9) in component form are simplified as

$$\tau_r = (\lambda^S + 2\mu^S)\frac{\partial u^S}{\partial r} + N\lambda^S\frac{u^S}{r}, \tag{14}$$

$$N\tau_\theta = N\left\{\lambda^S\frac{\partial u^S}{\partial r} + (N\lambda^S + 2\mu^S)\frac{u^S}{r}\right\}. \tag{15}$$

The initial and boundary conditions are

$$v^S(r,0) = v^F(r,0) = 0, \quad r > r_0, \tag{16}$$

$$\tau_r = -f(t) \quad \text{at } r = r_0, \tag{17}$$

where $f(t)$ is a function of time.

$$\text{Also } v^S, v^F \to 0 \quad \text{as } r \to \infty \tag{18}$$

Eq. (11) on integration and with the help of Eq. (18) provides

$$\eta^S v^S + \eta^F v^F = 0. \tag{19}$$

Eqs. (12) and (13) with the help of Eqs. (4) and (19) and also the stress–strain relations (14) and (15) yield

$$\eta^F \frac{\partial \tau_r}{\partial r} - \eta^F \rho^S \frac{\partial v^S}{\partial t} - \eta^S \eta^F \frac{\partial p}{\partial r} = S_V v^S - \frac{\eta^F N}{r}(\tau_r - \tau_\theta), \tag{20}$$

$$\eta^F \rho^S \frac{\partial v^S}{\partial t} - (\eta^F)^2 \frac{\partial p}{\partial r} = -S_V v^S, \tag{21}$$

$$\frac{\partial \tau_r}{\partial t} - (\lambda^S + 2\mu^S)\frac{\partial v^S}{\partial r} = N\lambda^S \frac{v^S}{r}, \tag{22}$$

$$N\left\{\frac{\partial \tau_\theta}{\partial t} - \lambda^S \frac{\partial v^S}{\partial r}\right\} = N(N\lambda^S + 2\mu^S)\frac{v^S}{r}. \tag{23}$$

Eqs. (20)–(23) form a system of four linear first-order partial differential equations with τ_r, τ_θ, v^S and p as dependent variables and r and t as the independent variables. These equations are fully hyperbolic and they permit the propagation of jumps in the partial derivatives of dependent variables along the characteristic directions, which are going to be presented in the next section.

4. Method of characteristics

The characteristic directions for the set of Eqs. (20)–(23) can be shown readily to be

$$\mathrm{I}^{\pm}: \ \frac{\mathrm{d}r}{\mathrm{d}t} = \pm c_0, \tag{24}$$

$$\mathrm{II}: \ \mathrm{d}r = 0. \tag{25}$$

The I^+ characteristic represents the line along which the discontinuities in the partial derivatives of the dependent variables propagate to the right and I^- is the path of propagation of these discontinuities to the left. The II characteristic is the degenerate case of dynamic wave at a given radial location. c_0 is the velocity of propagation and is given by

$$c_0 = \sqrt{\frac{(\eta^F)^2(\lambda^S + 2\mu^S)}{(\eta^F)^2\rho^S + (\eta^S)^2\rho^F}}. \tag{26}$$

If the pore liquid is absent or gas is filled in the pores, then ρ^F is very small as compare to ρ^S and can be neglected. So the relation (26) reduces to

$$c_0 = \sqrt{\frac{\lambda^S + 2\mu^S}{\rho^S}}. \tag{27}$$

This gives the velocity of a wave propagating in an incompressible porous solid, where the change in volume is due to the change in porosity and is a well-known result of the classical theory of elasticity. In an incompressible non-porous solid medium $\eta^F \to 0$, then again from Eq. (26) we have $c_0 = 0$ and is physically acceptable as a longitudinal wave cannot propagate in an incompressible medium.

The characteristic equations along $I^{\pm}$ are

$$(\eta^F)^2\,\mathrm{d}\tau_r \mp c_0\{(\eta^F)^2\rho^S + (\eta^S)^2\rho^F\}\,\mathrm{d}v^S = \left\{S_V v^S - \frac{N(\eta^F)^2}{r}\left(\tau_r - \tau_\theta \mp \frac{\lambda^S v^S}{c_0}\right)\right\}\mathrm{d}r \tag{28}$$

and the characteristic equation along II is

$$N\lambda^S\,\mathrm{d}\tau_r = -2N\mu^S\lambda^S\{(N+1)\lambda^S + 2\mu^S\}\frac{v^S}{r}\,\mathrm{d}t + N(\lambda^S + 2\mu^S)\,\mathrm{d}\tau_\theta. \tag{29}$$

These equations govern the propagation of discontinuities in the derivatives of x and v^S. Jumps also occur in the values of x and v^S as the wave propagates back and forth in the medium. To derive the analytical results for these discontinuities, we draw a characteristic of the family I^- and take two points P and Q on it which are sufficiently close to each other. Through these points, we draw the characteristics I_1^+ and I_2^+ of the family I^+ and also draw a characteristic PR of the family II as shown in Fig. 1(a). Integrating Eq. (28) for the lower sign from P to Q we get

$$(\eta^F)^2\{(\tau_r)_Q - (\tau_r)_P\} + c_0\{(\eta^F)^2\rho^S + (\eta^S)^2\rho^F\}\{(v^S)_Q - (v^S)_P\} = \int_P^Q A\,\mathrm{d}r.$$

Taking the limit as $Q \to P$ and as the integrand is bounded, so we have

$$(\eta^F)^2[\tau_r] + c_0\{(\eta^F)^2\rho^S + (\eta^S)^2\rho^F\}[v^S] = 0. \tag{30}$$

Similarly integration of Eq. (29) from P to R and in the limiting case as $R \to P$ yields

$$[\tau_r] = \frac{\lambda^S + 2\mu^S}{\lambda^S}[\tau_\theta]. \tag{31}$$

As the points P and Q are lying on the characteristics of the family I^+ so writing Eq. (28) for the upper sign along I_2^+ and I_1^+, subtracting one from the other and in the limiting case as $Q \to P$, we have

$$(\eta^F)^2\,\mathrm{d}[\tau_r] - c_0\{(\eta^F)^2\rho^S + (\eta^S)^2\rho^F\}\,\mathrm{d}[v^S] = \left\{S_V[v^S] - \frac{N(\eta^F)^2}{r}\left([\tau_r] - [\tau_\theta] - \frac{\lambda^S[v^S]}{c_0}\right)\right\}\mathrm{d}r.$$

This equation with the help of Eqs. (30) and (31) and on integration, yields

$$[\tau_r] = K\mathrm{e}^{-(L/2)r}r^{-(N/2)}, \tag{32}$$

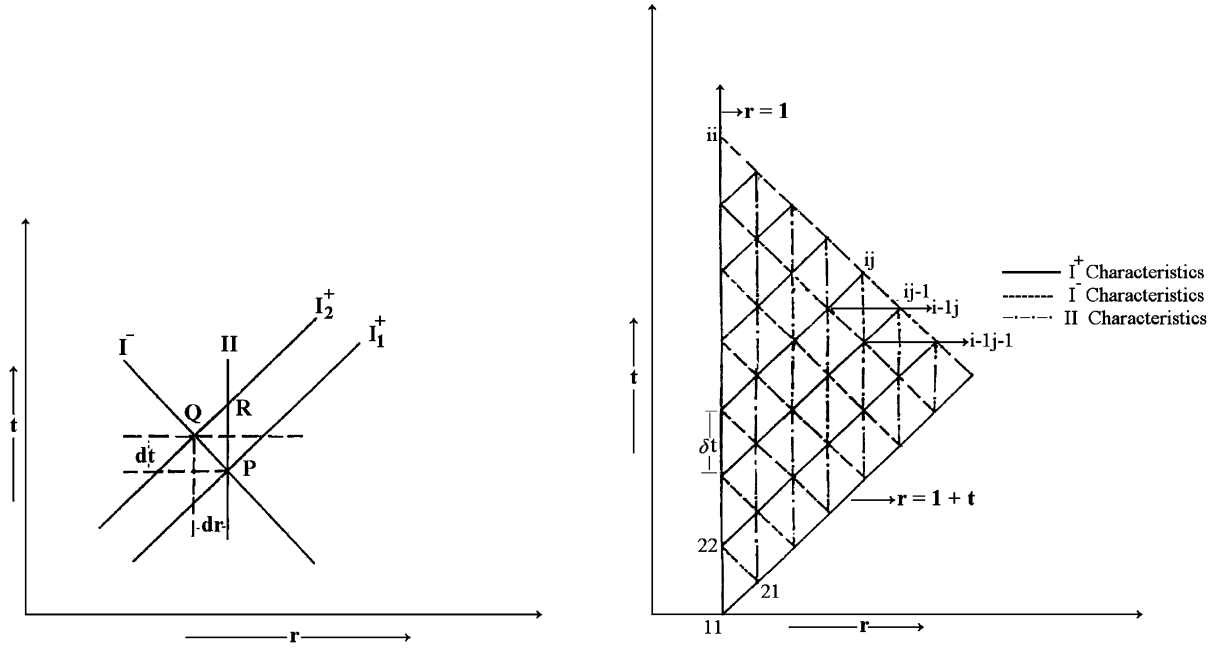

Fig. 1. (a) Propagation of discontinuities along I^+ characteristics and (b) characteristics network for numerical procedure.

where K is a constant and is evaluated by using the boundary condition and

$$L = \frac{r_0 S_V}{c_0\{(\eta^F)^2\rho^S + (\eta^S)^2\rho^F\}}. \tag{33}$$

Using the relation (32) in Eqs. (30) and (31) we get the equations for the variation of $[v^S]$ and $[\tau_\theta]$ as

$$[v^S] = -\frac{c_0}{(\lambda^S + 2\mu^S)} K e^{-(L/2)r} r^{-(N/2)}, \tag{34}$$

$$[\tau_\theta] = \frac{\lambda^S}{(\lambda^S + 2\mu^S)} K e^{-(L/2)r} r^{-(N/2)}. \tag{35}$$

Similarly the equations for the discontinuities across $dr/dt = -c_0$ are

$$[\tau_r] = K e^{-(L/2)r} r^{-(N/2)}, \tag{36}$$

$$[v^S] = \frac{c_0}{(\lambda^S + 2\mu^S)} K e^{-(L/2)r} r^{-(N/2)}, \tag{37}$$

$$[\tau_\theta] = \frac{\lambda^S}{(\lambda^S + 2\mu^S)} K e^{-(L/2)r} r^{-(N/2)}. \tag{38}$$

Using the incompressibility relation (19), we can easily derive the corresponding relations for discontinuities in particle velocity for fluid phase. If the pore liquid is absent then $S_V = 0$, so $L = 0$ and the relations (32)–(38) take the form

$$[\tau_r] = Kr^{-(N/2)}, \tag{39}$$

$$[v^S] = \mp \frac{c_0}{(\lambda^S + 2\mu^S)} Kr^{-(N/2)}, \tag{40}$$

$$[\tau_\theta] = \frac{\lambda^S}{(\lambda^S + 2\mu^S)} Kr^{-(N/2)}. \tag{41}$$

These results can also be compared with the well-known results of the classical theories, e.g. Ref. [5].

5. Numerical computation

Before presenting the numerical procedure, we introduce the non-dimensional quantities as

$$r' = \frac{r}{r_0}, \quad t' = \frac{c_0 t}{r_0}, \quad \tau'_r = \frac{\tau_r}{E}, \quad \tau'_\theta = \frac{\tau_\theta}{E}, \quad v^{S'} = \frac{(\lambda^S + 2\mu^S)}{E} \frac{v^S}{c_0}, \quad v^{F'} = \frac{(\lambda^S + 2\mu^S)}{E} \frac{v^F}{c_0},$$

where E is the Young's modulus of the solid phase, so that the results are true for any value of the physical parameters. The straight-line $r = 1 + t$ and $r = 1$ are the projections of the leading wave front and the straight-line $r = r_0$ in the new $r - t$ plane. We divide the straight-line $r = 1$ by a number of points in such a way that the distance between any two consecutive points is same throughout and is very small. Let this distance be δt and from the geometry of the characteristic lines, it is clear that $\delta r = \delta t$. Through these points we draw two families of the characteristic lines defined by Eq. (24) and then draw the characteristic lines of the family (25), joining their points of intersection as shown in the Fig. 1(b). The region between the straight line and $r = 1$ and $r = 1 + t$ is thus replaced by the discrete points as shown in the figure. The suffixes ij are attached to each grid point and it is clear that for any i; j varies from 1 to i and it provides a very good logic for the computer programming of the numerical technique. All these points can be divided into four categories. The point 11 is included in first category. It corresponds to the situation when the load is just applied and at this point all the quantities are known. The points lying on the straight line $r = 1 + t$ are included in the second category and as this straight line is a line of discontinuity, so the discontinuity relations are used to evaluate τ_r, τ_θ and v^S where as the geometry of the characteristics network provides the values of r and t. If $i1$ is any point of this category then

$$(\tau_r)_{i1} = K\mathrm{e}^{-(L/2)r_{i1}} (r)_{i1}^{-(N/2)}, \tag{42}$$

$$(v^S)_{i1} = \frac{c_0}{(\lambda^S + 2\mu^S)} K\mathrm{e}^{-(L/2)r_{i1}} (r)_{i1}^{-(N/2)}, \tag{43}$$

$$(\tau_\theta)_{i1} = \frac{\lambda^S}{(\lambda^S + 2\mu^S)} K\mathrm{e}^{-(L/2)r_{i1}} (r)_{i1}^{-(N/2)}, \tag{44}$$

$$t_{i1} = \left(\frac{i-1}{2}\right)\delta t, \tag{45}$$

$$r_{i1} = 1 + t_{i1}. \tag{46}$$

All the interior points are included in the third category. The values of r, t, τ_r, τ_θ and v^S at a typical interior point ij may be computed if all these quantities are known at the neighboring points $i-1j-1$, $ij-1$ and $i-1j$. Here the geometry of the characteristics net work provides the values of r and t. The corresponding characteristic equations are written in finite difference form and the quantities τ_r, τ_θ and v^S are evaluated from the algebraic equations so obtained. So we have

$$t_{ij} = t_{ij-1} + \tfrac{1}{2}\delta t, \tag{47}$$

$$r_{ij} = r_{ij-1} - \tfrac{1}{2}\delta t. \tag{48}$$

$$(\tau_r)_{ij} = \frac{P_1 + P_2}{2}, \tag{49}$$

$$(v^S)_{ij} = \frac{P_1 - P_2}{2}, \tag{50}$$

$$(\tau_\theta)_{ij} = (\tau_\theta)_{i-1\,j-1} + Q_2\{(\tau_r)_{ij} - (\tau_r)_{i-1\,j-1}\} + Q_3\delta t\frac{(v^S)_{i-1\ j-1}}{r_{i-1\ j-1}}, \tag{51}$$

where

$$P_1 = (\tau_r)_{i-1j} - (v^S)_{i-1j} + A_1(r_{ij} - r_{i-1j}), \tag{52}$$

$$P_2 = (\tau_r)_{ij-1} + (v^S)_{ij-1} + A_2(r_{ij} - r_{ij-1}), \tag{53}$$

$$A_1 = L(v^S)_{i-1j} - \frac{N}{r_{i-1j}}\{(\tau_r)_{i-1j} - (\tau_\theta)_{i-1j} - Q_2(v^S)_{i-1j}\}, \tag{54}$$

$$A_2 = L(v^S)_{ij-1} - \frac{N}{r_{ij-1}}\{(\tau_r)_{ij-1} - (\tau_\theta)_{ij-1} + Q_2(v^S)_{ij-1}\}, \tag{55}$$

$$Q_2 = \frac{\lambda^S}{Q_1}, \tag{56}$$

$$Q_1 = \lambda^S + 2\mu^S \tag{57}$$

and

$$Q_3 = \frac{2\mu^S\{(N+1)\lambda^S + 2\mu^S\}}{Q_1^2}. \tag{58}$$

Along the straight-line $r = 1$, where one of the variables is described remaining two may be determined from the two equations along I^- and II characteristics and these points are included in

fourth category and two suffixes are equal for these points. So we have

$$t_{ii} = (i-1)\delta t, \tag{59}$$

$$r_{ii} = 1, \tag{60}$$

$$(\tau_r)_{ii} = -f(t_{ii}), \tag{61}$$

$$(v^S)_{ii} = (v^S)_{ii-1} - (\tau_r)_{ii} + (\tau_r)_{ii-1} + A_3(r_{ii} - r_{ii-1}), \tag{62}$$

$$(\tau_\theta)_{ii} = (\tau_\theta)_{i-1i-1} + Q_2\{(\tau_r)_{ii} - (\tau_r)_{i-1i-1}\} + Q_3\delta t(v^S)_{i-1i-1}, \tag{63}$$

where

$$A_3 = L(v^S)_{ii-1} - \frac{N}{r_{ii-1}}\{(\tau_r)_{ii-1} - (\tau_\theta)_{ii-1} + Q_2(v^S)_{ij-1}\}. \tag{64}$$

Particle velocity for fluid phase is evaluated by using incompressibility relation (19). The pressure term neither appears in the equations of characteristic lines nor in the characteristic equations. This is due to the fact that the wave motion in porous medium may be expressed by the solid and fluid displacements or the solid extra stress but it cannot be expressed by the pore pressure, which of course is nothing else than the Langrangian multiplier corresponding to the incompressibility constraint of the binary medium. However, the pore pressure is evaluated from Eqs. (20) and (21) by eliminating the derivatives with respect to t and by writing the equations so obtained in difference form along the characteristic lines.

6. Discussion

For a particular model, we have taken Heaviside unit step input and the numerical values of the various physical parameters are taken from Boer and Ehlers [3]. Discontinuities in various quantities attenuate according to Eqs. (32)–(38). The variation of τ_r, τ_θ, v^S and v^F have been presented in Figs. 2–6. In particular the Figs. 2(a) and (b) show the solid velocity changing with respect to time and radial distance. It is evident that for a given r, the velocity of a solid particle decreases uniformly with time to some very small value. But if we consider the variation with respect to radial distance, we see that the velocities at all values of time approach to zero with increase of radial distance. Only difference is that for smaller value of time, the decrease is quick where as it is slow at large values of time. Figs. 4(a) and (b) show the variation of radial component of solid stress with respect to r and t. The magnitude of solid stress increase with time and approaches to its constant value at large values of time and so the curves are asymptotic to the straight line, $\tau_r = -1$, which represents the load applied at the cavity. Curves are drawn for three values of r and it is clear that the radial stress decrease with the increase of radial distance and it is again justified if we consider the variation with respect to radial distances at some fixed values of time Fig. 4(b). Here, starting from its maximum value which is 1 in our case, the magnitude of radial stress approaches very quickly to zero at small value of time but slowly at large values of time. Behaviour of circumferential component of stress, Figs. 5(a) and (b) is almost similar to that of radial component. The only difference is that the variation is small as compare

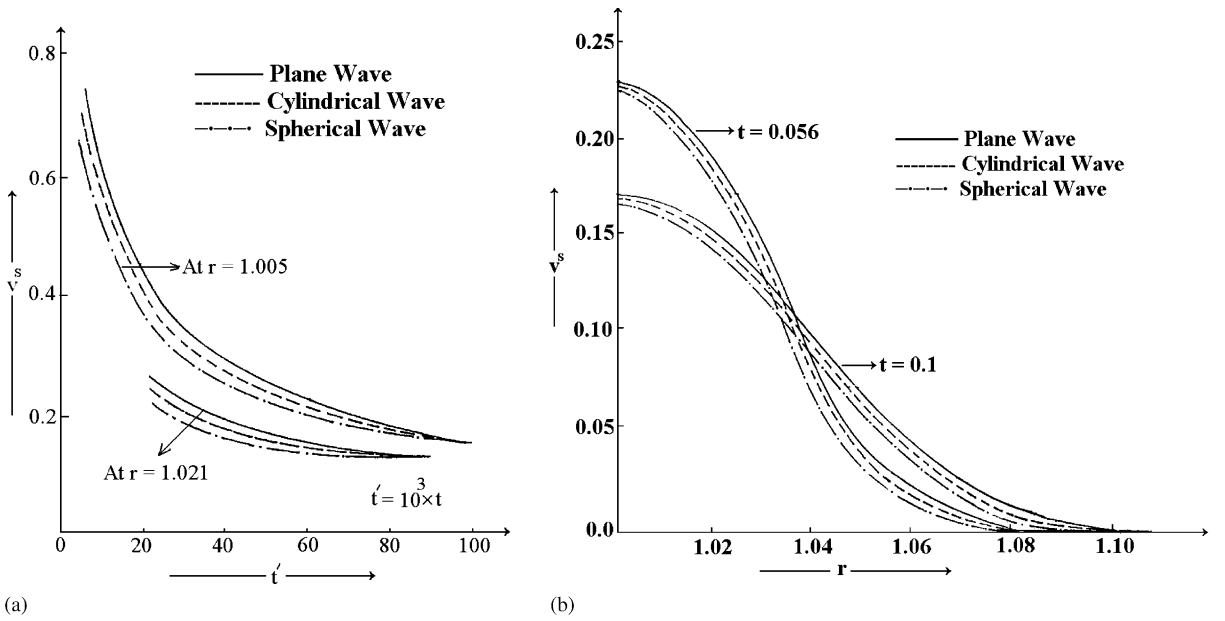

Fig. 2. Variation of v^S-versus (a) time and (b) radial distance.

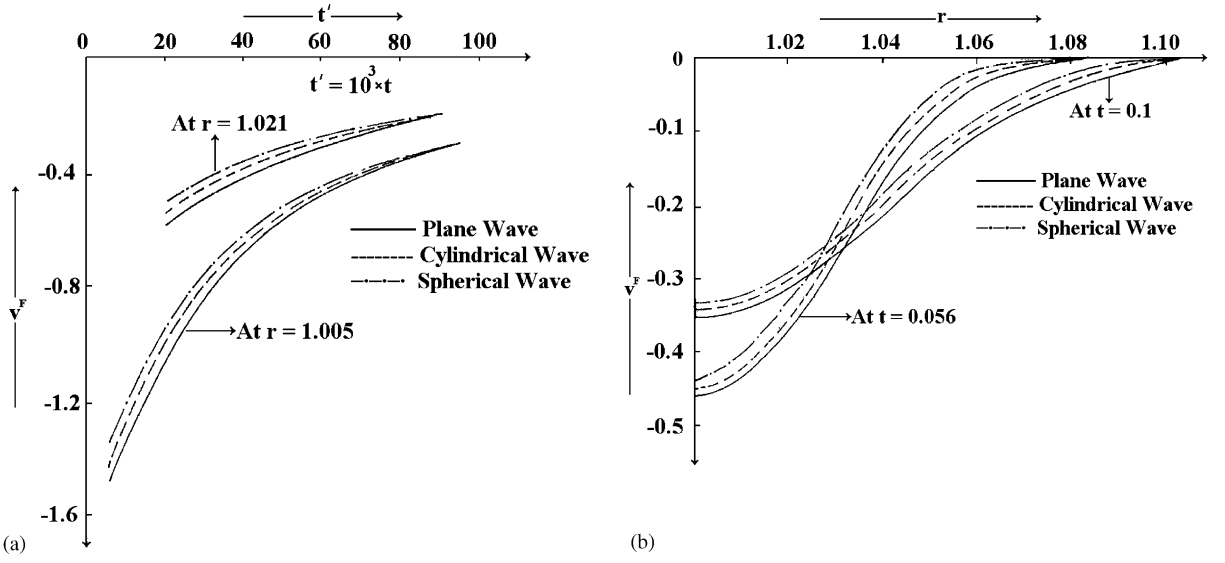

Fig. 3. Variation of v^F-versus (a) time and (b) radial distance.

to radial component. But one thing is very clear that the solid stresses increase with time at a given radial distance and decrease with distance from the loading surface at a given time. The pore pressure also decreases with time Fig. 6(a) and the trend of the curves show that the pores pressure

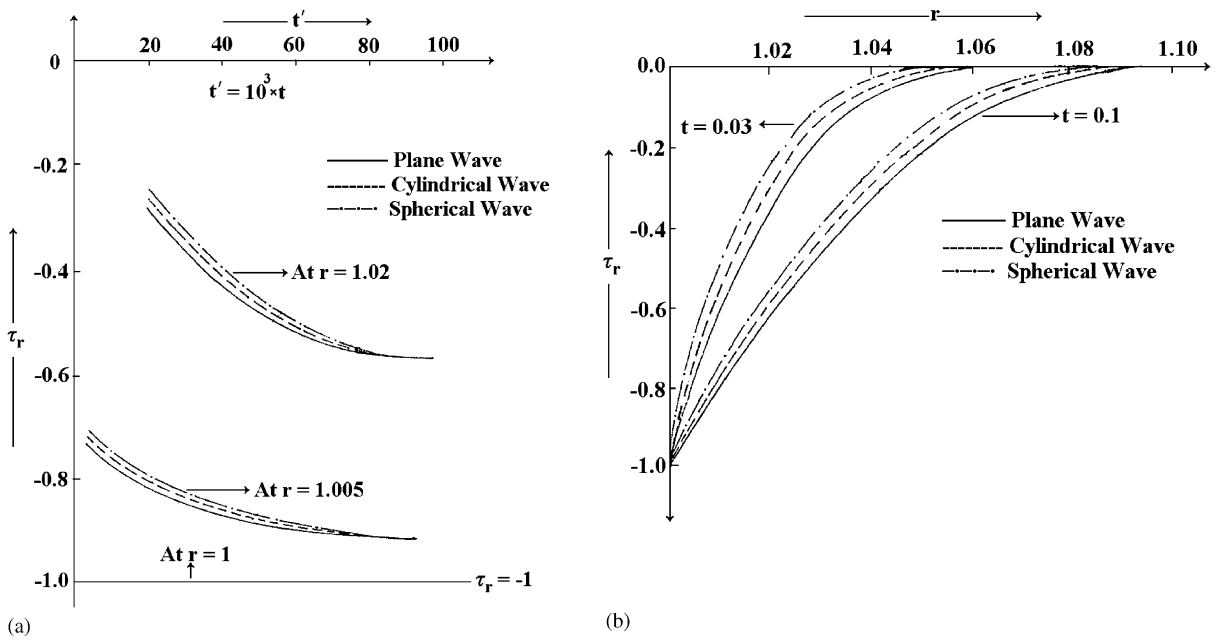

Fig. 4. Variation of radical component of solid stress versus (a) time and (b) radial distance.

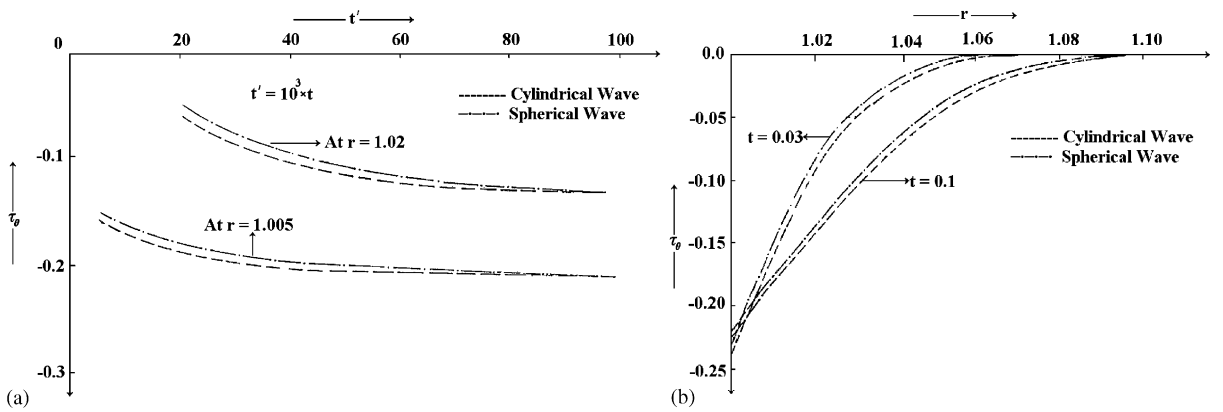

Fig. 5. Variation of circumferential component of solid stress versus (a) time and (b) radial distance.

at all the radii will approach to zero at large value of time. Unlike the stress, the pores pressure increases with radial distance very quickly near the cavity then increases gradually and ultimately becomes constant as shown in Fig. 6(b). As the result of incompressibility constraint, the motion of fluid phase is opposite to that of solid phase. That is why the graphs for fluid phase, Figs. 3(a) and (b), are the mirror images of the corresponding graph for solid phase. The magnitude of velocity of a fluid particle is greater than, equal to or less than that of the corresponding solid

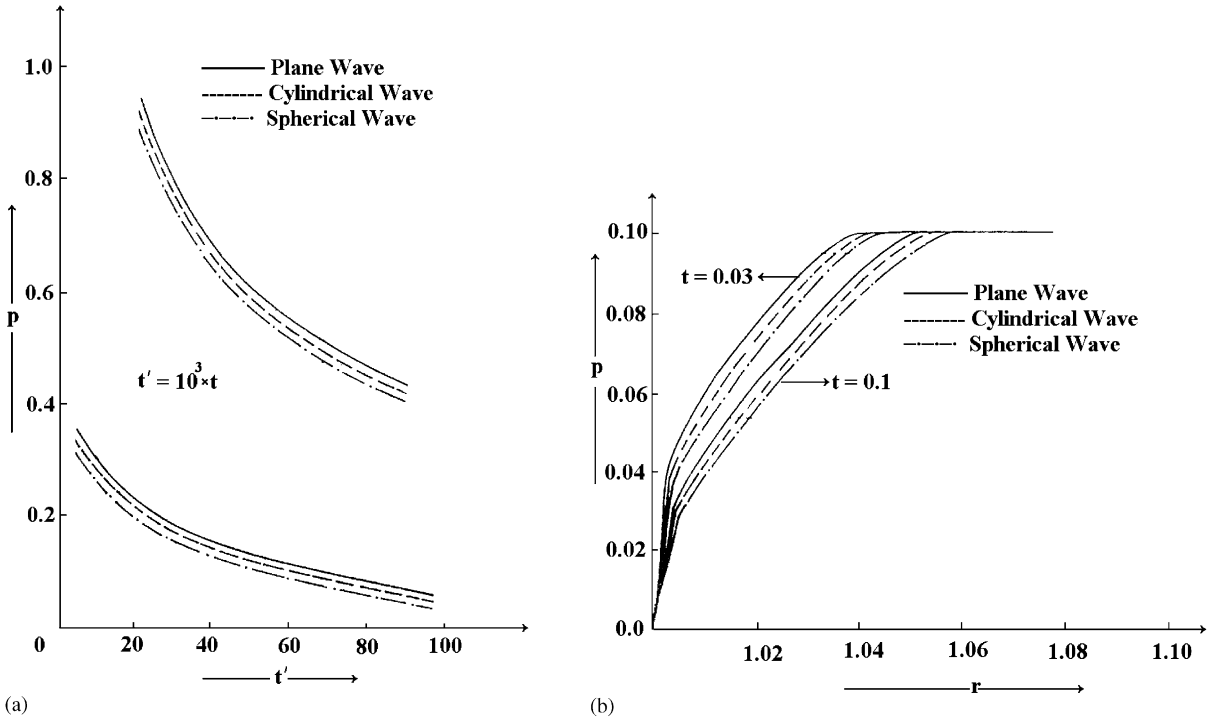

Fig. 6. Variation of pore pressure versus (a) time and (b) radial distance.

particle according as the quantity η^S/η^F is greater than, equal to or less than 1. Another important significance of the investigation is that, for the same medium and for the same input, the magnitude of the velocities, stresses and the pores pressure due to cylindrical wave is more than that due to spherical wave but less than that due to plane wave.

7. Conclusion

The propagation of plane, cylindrical and spherical waves in a fluid-saturated incompressible porous medium has been discussed. Saturated porous medium is modelled as two phase system with two incompressible constituents, where the general field equations are directly adopted according to the work of Boer and Ehlers [3]. The assumption of two incompressible constituents does not only meet the properties appearing in the many branches of soil mechanics, but it also avoids the introduction of many complicated material parameters as considered in the Biot theory. The governing partial differential equations are solved numerically using the method of characteristics. The incompressibility constraint exhibits only one wave propagating in both the solid and liquid phases. It has been observed that the discontinuities across the wave front are (i) inversely proportional to $e^{(L/2)r}$ for plane wave, (ii) inversely proportional to $e^{(L/2)r}$ and square root of the radial distance for cylindrical wave and (iii) inversely proportional to $e^{(L/2)r}$ and radial

distance for spherical wave. Heaviside step loading is taken for numerical investigation and the variation in various quantities, with time at various values of radial distance and with radial distance at various value of time is graphically presented.

References

[1] M.A. Biot, Theory of propagation of elastic waves in a fluid-saturated porous solid—I: low frequency range, *Journal of Acoustical Society of America* 28 (1956) 168–178.
[2] R.M. Bowen, Incompressible porous media models by use of the theory of mixtures, *International Journal of Engineering Sciences* 18 (1980) 1129–1148.
[3] R. de Boer, W. Ehlers, Uplift friction and capillarity—three fundamental effects for liquid-saturated porous solids, *International Journal of Solid Structures* 26 (1990) 43–57.
[4] R. de Boer, W. Ehlers, Z. Liu, One-dimensional transient wave propagation in a fluid-saturated incompressible porous media, *Archiv of Applied Mechanics* 63 (1993) 59–72.
[5] P.C. Chou, H.A. Koenig, A unified approach to cylindrical and spherical elastic waves by method of characteristics, *Journal of Applied Mechanics* 33 (1966) 159–167.
[6] P.C. Chou, R.W. Mortimer, Solution of one-dimensional elastic wave problems by the method of characteristics, *Journal of Applied Mechanics* 41 (1967) 745–750.
[7] P.C. Chou, P.F. Gordon, Radial propagation of axial shear waves in a non-homogeneous elastic media, *Journal of Acoustical Society of America* 42 (1967) 36–41.
[8] H.G. Hopkins, *Dynamic Expansion of Spherical Cavities in Metal. Progress in Solid Mechanics*, Vol. I, North-Holland Publishing Company, Amsterdam, Holland, 1960, pp. 84–164.
[9] O. Lekan, Vibration analysis of spherical shells, *International Journal of Engineering Sciences* 24 (1986) 1637–1654.
[10] V.P.W. Shim, S.E. Quah, Solution of impact induced flexural waves in a circular ring by the method of characteristics, *Journal of Applied Mechanics* 65 (1998) 569–579.
[11] R. Kumar, B.S. Hundal, A study of spherical and cylindrical wave propagation in a non-homogeneous fluid saturated incompressible porous medium by method of characteristics, in: P. Manchanda, et al. (Eds.), *Current Trends in Industrial and Applied Mathematics*, Anamya Publisher, New Delhi, 2002, pp. 181–194.
[12] R. Kumar, B.S. Hundal, Wave propagation in a fluid-saturated incompressible porous medium, *Indian Journal of Pure and Applied Mathematics* 4 (2003) 651–665.
[13] R. Kumar, B.S. Hundal, Effect of non-homogeneity on one-dimensional wave propagation in a fluid-saturated incompressible porous medium, *Bulletin of the Calcutta Mathematical Society* 96 (3) (2004) 179–188.
[14] R.J. Clifton, On a difference method for plane problems in dynamic elasticity, *Quarterly Applied Mathematics* 25 (1967) 97–116.
[15] M. Ziv, Two-spatial dimensional elastic wave propagation by the theory of characteristics, *International Journal of Solids Structures* 5 (1969) 1135–1151.
[16] M. Ziv, A general solution method for transient multi-dimensional problems in solid mechanics, *Bulletin of the Seismological Society of America* 65 (5) (1975) 1359–1384.
[17] P.R. Garabedian, *Partial Differential Equations*, Wiley, New York, 1964.
[18] R. Courant, D. Hilbert, *Methods of Mathematical Physics*, Vol. II, Wiley Eastern Private Limited, New Delhi, 1975.
[19] A. Jefferey, T. Taniuty, *Non-linear Wave Propagation*, Academic Press, New York, 1964.
[20] I.N. Sneddon, *Elements of Partial Differential Equations*, McGraw-Hill Book Company Inc., New York, 1957.